

doi: 10.18720/MCE.84.1

## Rational use of HPSFRC in multi-storey building

Возможность рационального использования HPSFRC  
в многоэтажном строительстве

*K. Buķa-Vaivade,  
J. Sliseris,  
D. Serdjuks\*,  
L. Pakrastins,  
Riga Technical University, Riga, Latvia  
N.I. Vatin,  
Peter the Great St. Petersburg Polytechnic  
University, St. Petersburg, Russia*

*М.С., научный сотрудник К. Бука-Вайваде,  
д-р техн. наук, ассоц. профессор  
Я. Шлисери́с,  
д-р техн. наук, профессор Д.О. Сердюк\*,  
д-р техн. наук, руководитель кафедры  
Л. Пакрастиньш,  
Рижский технический университет, г. Рига,  
Латвия  
д-р техн. наук, профессор Н.И. Ватин,  
Санкт-Петербургский политехнический  
университет Петра Великого,  
Санкт-Петербург, Россия*

**Key words:** high-performance concrete; high-performance steel fibre reinforced concrete; stress–strain curve; elements of multi-storey building

**Ключевые слова:** высокопрочный бетон; высокопрочный сталефибробетон; кривая напряжение-деформация; элементы многоэтажного здания

**Abstract.** Fibres improve concrete properties that can be used to solve the problem of limited resources. This research includes the numerical comparison of high-performance concrete (HPC) and high-performance steel fibre reinforced concrete (HPSFRC) behaviour. The numerical comparison is based on the analyse of stress-strain curves of considered materials. The limits of rational use of HPC and high-performance steel fibre reinforced concrete HPSFRC have been determined based on typical stress resultants values acting in the elements of multi-storey buildings. The values of stress resultants were determined by the numerical model, which was developed by the software ANSYS. Interaction diagrams of bending moments and axial forces  $M-N$  for elements subjected to combined action of compression and bending with different cross-sections have been developed. Curves for slabs of two material types that describe the allowable values of distributed load at different spans of the slabs are created. The resulting curves are analysed together with the actual stress resultants of the elements concerned from the numerical model. Taking into account distribution of stress resultants in the elements of multi-storey buildings, it was stated that the elements subjected to flexure are preferable field of application for HPSFRC. Ultimate value of bending moment is higher for HPSFRC comparing to HPC with the same parameters of cross-section. It is found that it is more rational to use HPSFRC for columns in the first eight floors. HPSFRC should be preferred as a material of the lower and middle floors of multi-storey buildings and of the walls of all floors in the case of column spacing more than 8 m, and for the slabs with span interval 6–12 m.

**Аннотация.** Поскольку введение фибры приводит к улучшению свойств бетона, это может быть использовано для решения проблемы ограниченности ряда строительных материалов. Данное исследование включает в себя численное сравнение работы бетона высокой прочности (НПС) и бетона высокой прочности со стальной фиброй (HPSFRC). Сравнение основывается на анализе кривых «напряжения–деформации» данных материалов. Границы более рационального использования бетонов НПС и HPSFRC определяются на основе типовых значений внутренних усилий в конструкциях многоэтажных зданий, полученных на основе разработанной в среде ANSYS численной модели. Получены диаграммы взаимосвязи изгибающих моментов и осевых сил  $M-N$  для внецентренно сжатых элементов с различными поперечными сечениями. Диаграммы, полученные для плит из двух исследуемых материалов, демонстрируют допустимые значения распределенной нагрузки для плит различных пролетов. Анализ полученных диаграмм проводится с учётом внутренних усилий соответствующих элементов из численной модели. В результате проведенной работы установлено, что при тех же параметрах поперечного сечения конструкции, выполненные из бетона HPSFRC, способны воспринимать более высокие значения изгибающего момента, чем конструкции на основе НПС. Выявлено, что наиболее рационально использовать HPSFRC для колонн первых восьми этажей. В качестве строительного материала для колонн

Бука-Вайваде К., Шлисери́с Я., Сердюк Д.О., Пакрастиньш Л., Ватин Н.И. Возможность рационального использования HPSFRC в многоэтажном строительстве // Инженерно-строительный журнал. 2018. № 8(84). С. 3–14.

нижних и средних этажей и всех стен ядра жесткости при шаге колонн более 8 м, а также для плит с пролетом в интервале от 6 до 12 м рекомендуется использовать HPSFRC.

## 1. Introduction

The number of people in the world is growing rapidly, according to the U.S. Census Bureau, every minute, the population of the planet is growing by an estimated 150 people, accounting for more than 80 million people per year. As a result, two issues remain: living space – there is a need for multi-storey buildings and availability of natural resources. The principle of sustainable development aims to preserve the environment and nature for future generations at least in the same quality as we have received. As stocks of non-renewable resources decrease every year, it is important to use these resources economically and rationally, with the greatest possible efficiency. This approach also applies to the construction industry.

The constructive solution of a multi-storey residential building with load-bearing structures from thin-walled high-performance concrete (HPC) or high-performance steel fibre reinforced concrete (HPSFRC) avoids the large vertical cross-sectional structure of the building on the lower floors [1–3]. This will allow us to reduce the self-weighting of structures, increase the useful area and save on non-renewable natural resources.

The use of fibres improves the properties of concrete especially in tension loads. This improvement depends on many factors: fibre shape, the ratio between fibre length and its equivalent diameter or aspect ratio  $l_f / d_f$ , fibre volume etc. [3–10]. Therefore, predicting the properties of fibre reinforced concrete is complicated. However, investigations have shown that the improvement of the strength of concrete from the use of fibres is usually negligible and not observed [11], while the fibres distribute localized stress, prevent the cracking of concrete, improve ductility of high-performance concrete and significantly improve the post-peak behaviour of the fibre reinforced concrete [8–19], as a result reduces the cost of maintenance and repair. When the first crack appears in concrete, fibres begin to work, fibre bridging effect affects the deformation properties of the concrete [3, 6, 9, 11].

There are many studies [3, 6, 9, 20–22] where stress-strain curves of the concrete with and without steel fibre reinforcement are experimentally obtained. The obtained stress-strain curves prove the significant increase in post-peak stage of permissible strain values, moreover, fibres can significantly reduce shrinkage of concrete. Dimensions of cross-sections and ratio of longitudinal reinforcement for load-bearing members of multi-storey building subjected to flexure and compression with the bending probably can be decreased due to this property of HPSFRC. As a consequence of this the use of HPSFRC can reduce the cost of labour and the delivery of bars. So, the aim of this investigation is to compare numerically the behaviour of HPC and HPSFRC with steel fibre dosage 25–35 kg/m<sup>3</sup>, and to evaluate the limits for effective use of HPSFRC. Distribution of the typical stress resultants acting in the elements of a multi-storey building with different column spacing should be analysed for this purpose. The task of the study is to determine the boundaries of the effective use of HPSFRC columns, walls and ribbed slabs. The field of application of the results obtained is the initial design stage, during which it is necessary to select the used structures and materials.

Load bearing capacity diagrams for combined bending and axial load for columns and walls of different sizes will be developed in this research. Curves characterizing the load-bearing capacity of ribbed slabs with different slab parameters and the parametric numerical model of the building for determining the typical work of the building will be created also.

## 2. Methods

### 2.1. Object of investigation

A multi-storey building (Figure 1) with a stiffness core walls in the centre and perimeter columns, providing self-supporting exterior walls and ribbed slabs, was considered as an object of this investigation. The columns cross-sections are selected as a box-type to provide the decreased consumption of materials and high stiffness of the element in the both planes. The box-type cross-section enables the integration of engineering communication inside or outside of columns.

### 2.2. Numerical model of the building

3D numerical model of the multi-storey building is developed by the ANSYS software. The parametric design language (APDL) of ANSYS software is used to automate the design process by defining geometry with relationships, variable parameters and criteria, and to create a parametric model.

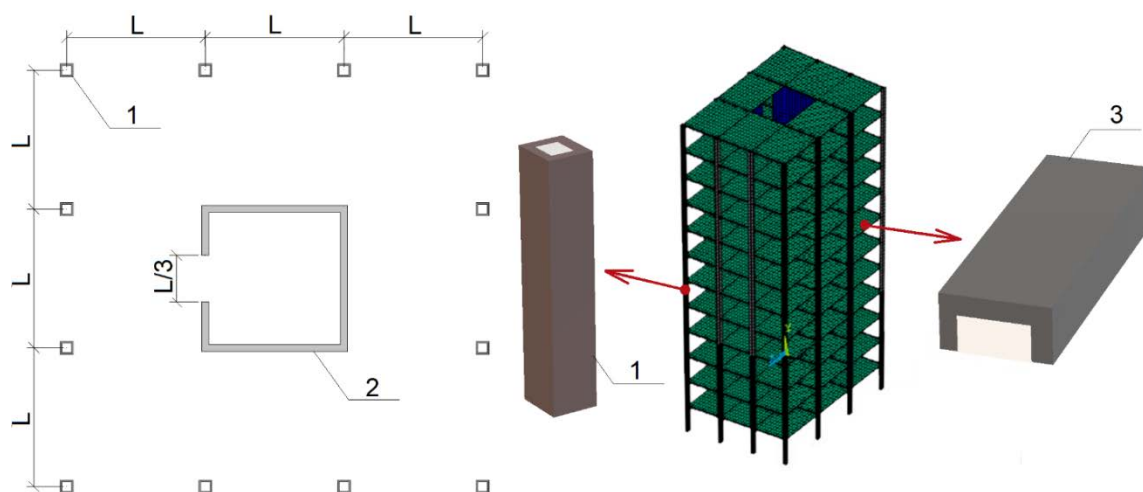


**Figure 1. Structure of considered multi-storey building. 1 – columns, 2 – walls, 3 – ribbed slabs.**

The building calculation model is developed with the ability to modify input data such as the column spacing ( $L$ ), floor height ( $h$ ), number of storeys ( $n$ ), concrete strength and cross-sectional parameters of the elements. A building with twelve storeys is considered. The height of the storey is equal to 4 m and the column spacing changes within the limits from 6 to 13 m. The columns of the first storey are rigidly joined with the foundation as the supports of the model are considered as completely fixed from the linear displacements and rotations. A concrete core walls are created to ensure the rigidity of the building.

Structures of slabs and walls are modelled by the SHELL181 finite element type, while the columns and beams by the finite element type BEAM188. The transversal deformation is taken into account for both of considered type of elements [23].

Dimensions of the walls and columns cross-sections are defined parametrically. They are divided into three groups and changes for the storeys: from the 1st to the 4th storeys there is a first group, from 5th to 8th storey there is a second storey group and from the 9th to 12th storey there is a third storey group. Column cross-section is box-type, with constant external dimensions. It is 500×500 mm and variable wall thickness. Pinned support is modelled for the slabs by the degrees of freedom Coupling function, it allows rotation and prevent the translation movements.

The obtained model is analysed based on a constant load combination of permanent load, uniformly distributed imposed load 5 kN/m<sup>2</sup>, which is applied to the all floors, including roof and wind load, which is applied as linear load to the columns of one of the facades. Openings are not taken into account. The created numerical model enables to determined forces of the building elements at different column spacing.

### 2.3. Modelling of structural materials

Three types of materials are used in the design model of the building, i.e. high-performance concrete, high-performance steel fibre reinforced concrete and steel. High-performance concrete is characterized as a brittle material. The structural members made of concrete have at least minimum reinforcement. High strength concrete of C80 / 95 class is used [24]. Improvement in peak strength due to the use of fibres is not respected, as it is usually negligible, while the improved of post-peak behaviour of the concrete is taken into account. For the high-performance steel fibre reinforced concrete are used steel fibres with length 50 mm, diameter 1 mm and dosage 25–35 kg/m<sup>3</sup>.

HPC and HPSFRC are approximated by using discrete lattice model to describe non-linear and discrete nature of concrete. Lattice model is obtained from standard tetrahedron finite element mesh, where each lattice member is edge of tetrahedron. The behaviour of non-linear material is characterized by degradation of Young's modulus cause of cracking. Damage variable is used for the prediction of behaviour of HPC and HPSFRC [25]:

$$E = E_{init} \cdot (1 - D),$$

where  $E_{init}$  – the initial material Young's modulus,

$D$  – a damage variable (0 – undamaged, 1 – damaged material).

To obtain the dependences of the bending moments on the axial forces  $M-N$ , the axial load is applied in 10 steps from 0 to the maximum bearing capacity in compression. For each step, the maximum value of the bending moment, which can be additionally applied to an axial force, is determined iteratively. Numerical modelling approach in more detail is described in [25–29].

Used stress-strain curves of the materials [3, 4, 23, 30] are shown in Figures 2 and 3.

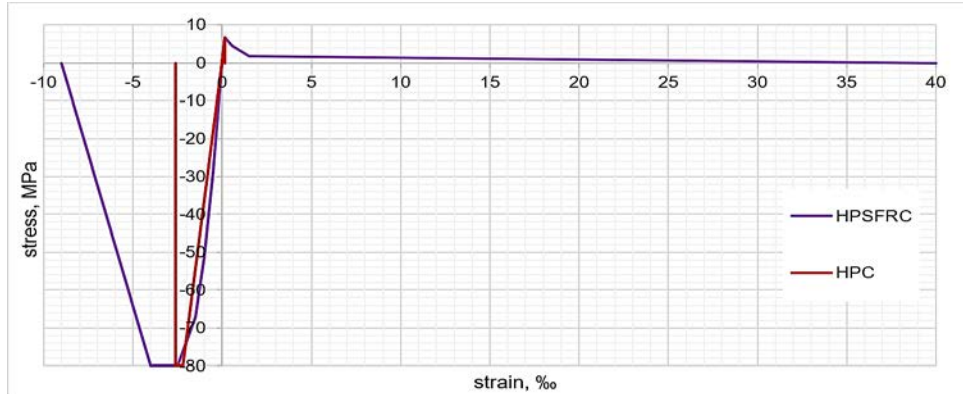


Figure 2. Stress-strain curve of high-performance concrete (HPC) and high-performance steel fibre reinforced concrete (HPSFRC).

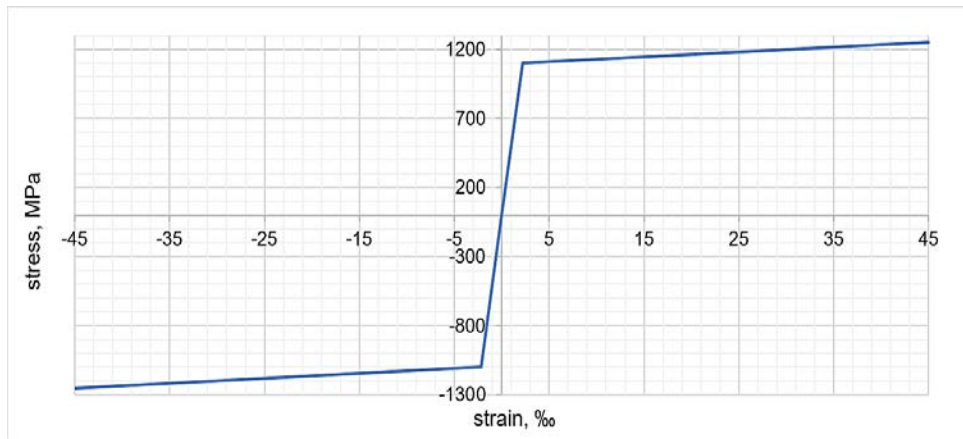


Figure 3. Stress-strain curve of high-strength steel.

Values of stress-strain curves of the HPC and HPSFRC are given in the Table 1.

Table 1. Stresses values of HPC and HPSFRC as a function from the strains.

strain, ‰		-9.0	-4.0	-2.6	-2.2	-1.5	0.0	0.14	0.16	1.50	40.0
stress, MPa	HPC	0	0.0	0.0	80.0	80.0	54.5	0.0	6.8	0.0	0.0
	HPSFRC	0	80.0	80.0	80.0	80.0	67.2	0.0	6.8	6.7	1.8

Values of stress-strain curves of the high-strength steel (HSS) are given in the Table 2.

Table 2. Stresses values of HSS as a function from the strains.

strain, ‰	-45.0	-2.2	0.0	2.2	45.0
stress, MPa	-1250	-1100	0.0	1100	1250

#### 2.4. Analysis of elements behaviour

Interaction diagrams  $M-N$  for columns and walls and load-bearing curves for slabs for different cross-sectional dimensions have been developed by the analysis of HPC and HPSFRC. The resulting diagrams include the maximum values of stress resultants obtained by the developed numerical buildings model. The diagrams enable to find out the limits for the rational use of HPC and HPSFRC.

The height of the building is divided into three groups, as it was mentioned in the Chapter 2. The thickness of the core walls and of the column box-type cross-section walls may vary for each group.

The ribbed slabs are analysed by using uniformly distributed load, which include permanent and imposed loads. The characteristic value of imposed load is  $5 \text{ kN/m}^2$ . The width of the ribbed slab, which is considered as a specimen used for comparison of HPC and HPSFRC, was equal to 1 m.

The minimum thickness of the concrete protective layer for reinforcement is  $c_{nom,min} = 20 \text{ mm}$  [24]. Then the width of the rib of the slab ( $b_w$ ) is:

$$b_w = \begin{cases} 2 \cdot c_{nom,min} + \varnothing = 2 \cdot 20 + \varnothing = 40 + \varnothing \text{ mm} - \text{pie } \varnothing \leq 10 \text{ mm}, \\ 2 \cdot (\varnothing + 10) + \varnothing = 20 + 3 \cdot \varnothing \text{ mm} - \text{pie } \varnothing > 10 \text{ mm}, \end{cases}$$

where  $\varnothing$  is diameter of longitudinal bar.

The width of the slab is rounded up by 10 mm in the calculations.

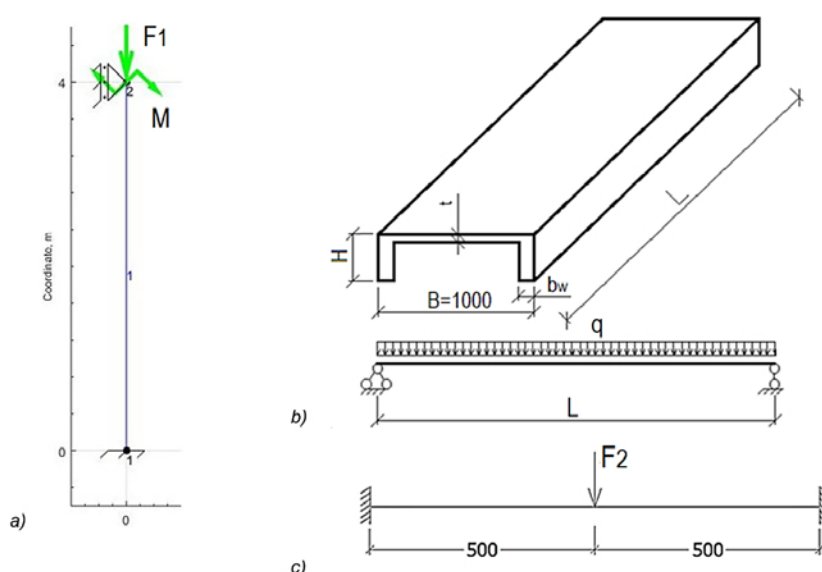


**Figure 4. Design schemes of a) columns and walls elements subjected to compressive force; b) height ( $H$ ) of the ribbed slabs and main geometric characteristics of ribbed slabs; c) thickness ( $t$ ) of the slabs web.**

The design schemes of the elements subjected to compression and the bending are shown in Figure 4. The thickness of the slab ( $t$ ) is determined by loading the web of the slab with a concentrated force (Figure 4 (c)) for two cases – a slab of HPC and HPSFRC.

Comparison of load bearing capacity of the HPC and HPSFRC slabs was carried out. Calculations of slab deflections have been also done considering that the serviceability limit state is determinant for elements in bending. The deflection in the middle of the span of the ribbed slab is calculated by taking into account permanent and imposed loads and by using material stress-strain curves. The maximum available deflection is taken as  $1/250$  part of the span.

### 3. Results and Discussions

#### 3.1. Columns behavior

The maximum axial forces and bending moments for the columns of all three groups with the distance between column centres equal to 8 m and for the columns of the first group with the spacings equal to 6 m are summarized in the Figure 5. The values of the axial forces and bending moments were obtained by the 3D model of the building, which was developed by the software ANSYS. Figure 5 include the interaction diagrams  $M-N$  for combined bending and axial load for the HPC and HPSFRC columns with box-type cross-sections and wall thicknesses equal to 50 and 60 mm.

Бука-Вайваде К., Шлисериц Я., Сердюк Д.О., Пакрастиныш Л., Ватин Н.И. Возможность рационального использования HPSFRC в многоэтажном строительстве // Инженерно-строительный журнал. 2018. № 8(84). С. 3–14.

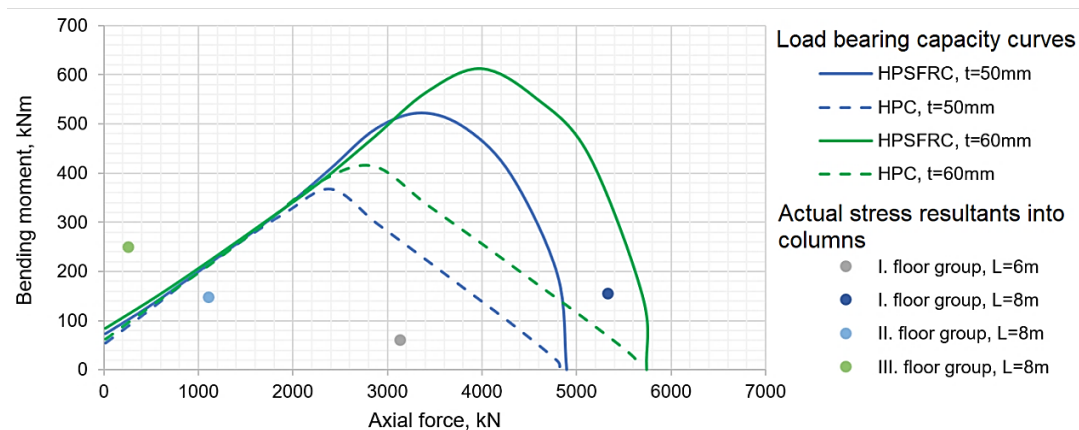


**Figure 5. Dependences of the bending moments on the axial forces  $M-N$  for the HPC and HPSFRC columns, with box-type cross-section and wall thicknesses equal to 50 and 60 mm.**

As can be seen from Figure 5, the character of the dependences of the bending moments on the axial forces for HPC and HPSFRC are similar while the dependences for HPC reached its maximum bending moment. The maximal axial force in compression is also comparable for both materials. Behaviour of HPSFRC varies greatly with the growing of axial force and bending moment values. After reaching the peak bending moment of a HPC, this difference grows till 40–90 %.

Columns of the third storey group are characterized by a high bending moment value at low axial force, as a result, firstly, in order to ensure the load bearing capacity of the columns, these columns need an additional longitudinal reinforcement; secondly, considering that the character of behaviour of HPSFRC and HPC is not significantly different at low axial force values, it can be concluded that using of HPC for the columns of the third storey group enables to increase effectiveness of the structural materials use.

It is accepted that the thickness of the column box-type cross-section wall must be bigger than 50 mm due to the technological considerations. Then it can be seen that the material is not used rationally at the small column spacing, thereby HPC is sufficient to provide the bearing capacity of the columns.

The columns of the first group of the storeys for building with column spacing equal to 8 m are characterized by a relatively high bending moment value at a high axial force, resulting the load bearing capacity of the column with a uniform thickness of the box-type cross-section wall ( $t = 60$  mm) can be provided by using of HPSFRC as the column material instead of HPC.

The maximum values of axial forces and bending moments for the columns of the first and second group of storeys are summarized in the Table 3 for columns spacings changing within the limits from 11 to 13 m.

**Table 3. Maximum values of axial forces and bending moments for the different columns spacings.**

Storeys	$L = 11$ m		$L = 12$ m		$L = 13$ m	
	$N$ , kN	$M$ , kNm	$N$ , kN	$M$ , kNm	$N$ , kN	$M$ , kNm
1–4	9874.8	613.6	11570	850.6	13454	1175
	9874	642.2			12429	1154.8
5–8	6534.4	32.3	7664.4	32.3	8929.4	5.8
	6011	387	7108.7	521.2	8426.3	722.4

The dependences of the bending moments on the axial forces  $M-N$  for HPSFRC and HPC columns with box-type cross sections, which are differed by thicknesses of the walls so as amount and diameters of the longitudinal bars, is shown on the Figure 6. The values of stress resultants are obtained by the 3D numerical model of the building.

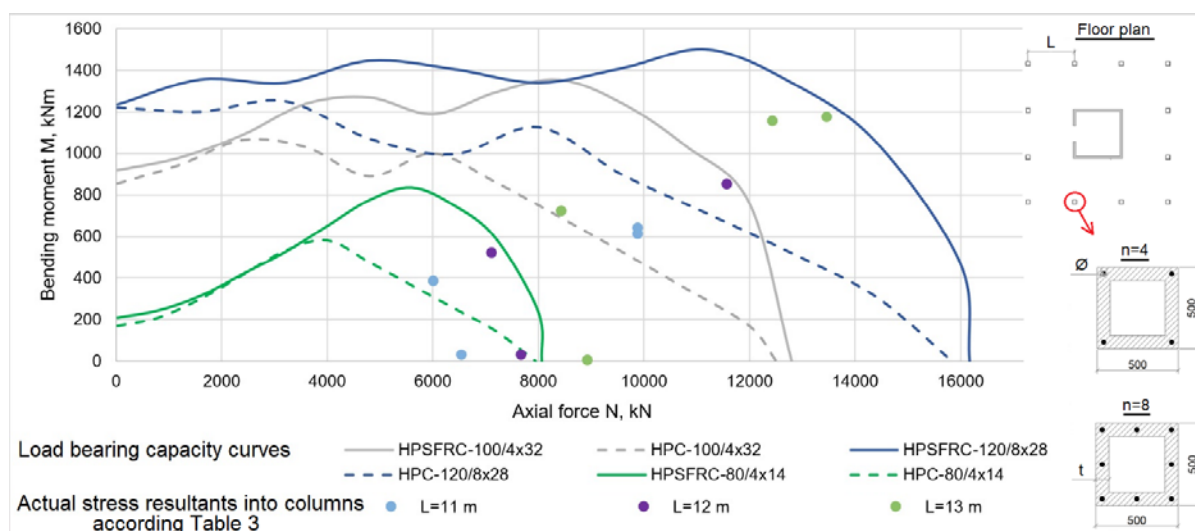


**Figure 6. Dependences of the bending moments on the axial forces  $M-N$  for HPSFRC and HPC columns for the first and second groups of storeys with box-type cross-sections.  $t/n \times \emptyset$ :  $t$  is box-type cross-section wall thickness,  $n$  is number of longitudinal bars in cross-section,  $\emptyset$  is diameter of longitudinal bars.**

It can be concluded, that the use of HPSFRC as column material for the first and second storey group is justified. For example, maximum value of bending moment in the column of the first storey group is 851 kNm and of the second group is 521 kNm for building with column spacing equal to 12 m. HPSFRC columns with box-type cross-section 100/4×32 and 80/4×14, respectively, provide load bearing capacity, while 3.3 times smaller value of the bending moment can be taken up at the same parameters of cross-section HPC columns. As it shown in Figure 6, cross-section 100/4×32 of HPC column is needed to provide 521 kNm big bending moment. In this case, it means 25 % thicker wall of box-type cross-section or about 245 kg more concrete per one column and 2.28 times bigger diameter of bars or 0.13 tonnes more steel per one column. It means, that HPSFRC allows to considerably reduce cross-section size and diameter of longitudinal bars.

The required thicknesses of the walls so as amount and diameters of the longitudinal bars ( $t/n \times \emptyset$ ) for cross sections of columns when the columns spacings changing within the limits from 11 to 13 m are summarized in the Table 4.

**Table 4. HPSFRC column cross sections ( $t/n \times \emptyset$ ) at different column spacing.**

$L, m$	11	12	13
I. storey group	100/4X32	100/4X32	120/8X28
II. storey group	80/4X14	80/4X14	100/4X32

### 3.2. Walls behavior

The dependences of the bending moments on the axial forces  $M-N$  for HPSFRC and HPC walls with thickness 90 mm, with and without additional reinforcement, are shown on the Figure 7.

As can be seen, the stage in which the wall can take up both the axial force and the bending moment, for HPSFRC walls is significantly higher. The values of bending moment, which can be taken up by the wall, at corresponding values of axial forces, for HPSFRC are 20–100 % higher, than for HPC.

It can be seen from the Figure 7, that the minimum additional reinforcement significantly increases the value of the bending moment that can be applied to the wall unloaded by the axial force.

The maximum values of bending moments and axial forces, acting in the walls of the different storeys groups for buildings with column spacing of 8 and 12 m, according to 3D numerical model, is summarized in Table 5.

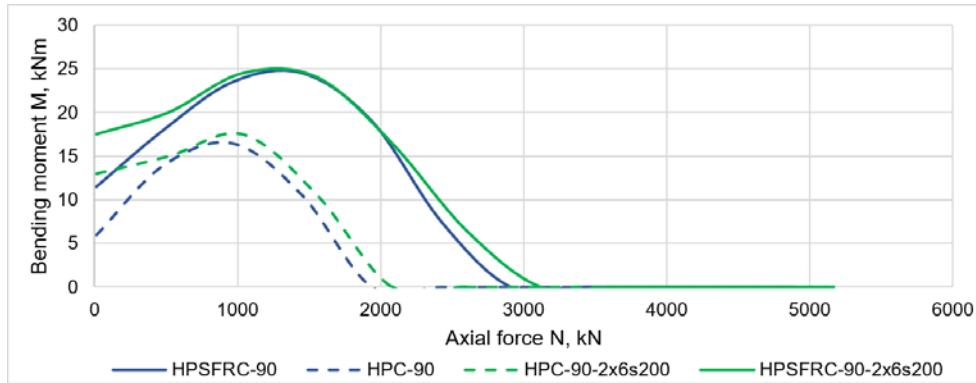


**Figure 7. Dependences of the bending moments on the axial forces  $M-N$  for walls with/without additional two-way reinforcement. HPSFRC is high-performance steel fibre reinforced concrete; HPC is high-performance concrete; -90 is wall thickness, 2×6s200 is two two-way slab reinforcement with bars spacing 200×200 and diameter 6 mm.**

**Table 5. Maximum values of bending moments and axial forces, in the walls of the different storeys groups.**

Storeys	$L = 8\text{ m}$		$L = 12\text{ m}$	
	$N$ , kN	$M$ , kNm	$N$ , kN	$M$ , kNm
1-4	2236.1	12.0	4666.9	36.6
	2024.6	13.1	2770.0	42.1
5-8	1950.2	13.4	4217.3	37.6
	1700.3	14.1	927.2	41.06
9-12	1609.0	13.9	3808.1	38.9
	1392.2	14.7	671.4	47.7

Maximal forces from the 3D numerical model of the building are plotted together with the dependences of the bending moments on the axial forces  $M-N$  for walls with different thicknesses are shown on the Figure 8.

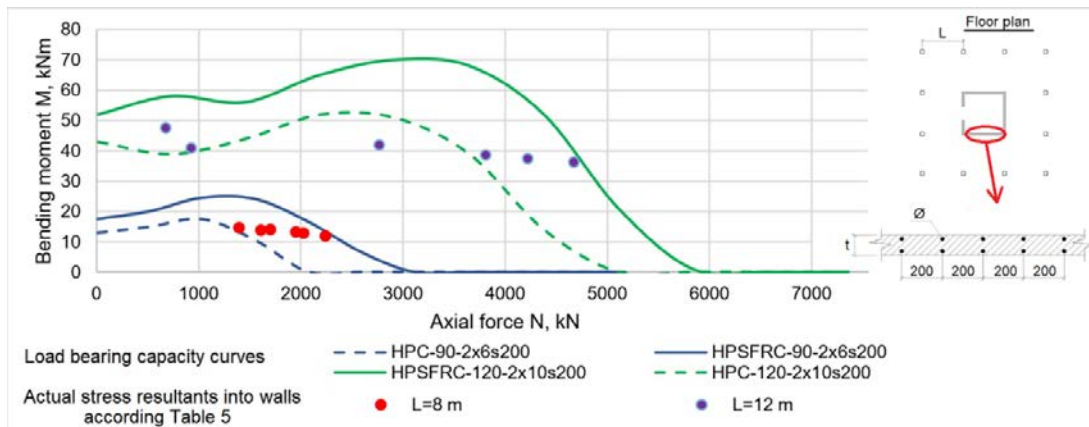


**Figure 8. Dependences of the bending moments on the axial forces  $M-N$  for walls. HPSFRC is high-performance steel fibre reinforced concrete; HPC is high-performance concrete; -90, -120 are wall thickness ( $t$ ), 2×6s200 is two two-way slab reinforcement with bars spacing 200×200 and diameter  $\varnothing = 6\text{ mm}$ , 2×10s200 is two two-way slab reinforcement with bars spacing 200×200 and diameter  $\varnothing = 10\text{ mm}$ ;  $L = 8\text{ m}$ ,  $L = 12\text{ m}$  are maximal forces in walls at the appropriate column spacing.**

The maximum values of axial forces and bending moments in the walls does not have such a sharp difference in the storey groups. So, the use of HPSFRC is justified for the core walls of the buildings with various column spacing.



### 3.3. Slabs behavior

The dependence of the maximum bending moment, acting in the middle of the web span of the ribbed slab, from the thickness of the web is shown on the Figure 9. It can be seen from the Figure 9 that the bending moment that can be taken up by the HPSFRC slab web is 38 ... 41 % higher than that for slab web of HPC, with the same thickness of the slab web.

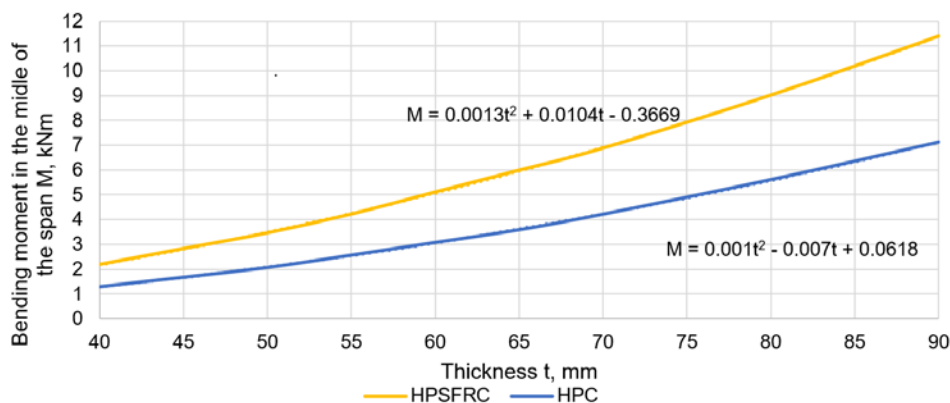


**Figure 9. The dependence of the maximum bending moment, acting in the middle of the web span of the ribbed slab, from the thickness of the web ( $t$ ), HPSFRC is high-performance steel fibre reinforced concrete; HPC is high-performance concrete.**

Thickness of the slabs webs is rounded up by 5 mm due to technological limitations of manufacturing. Then the thickness of the web, which will provide a load bearing capacity of  $F = 20$  kN ( $M \approx 2.5$  kNm with web span 1 m), for HPSFRC is 45 mm, while for HPC it is 55 mm at the same load bearing capacity.

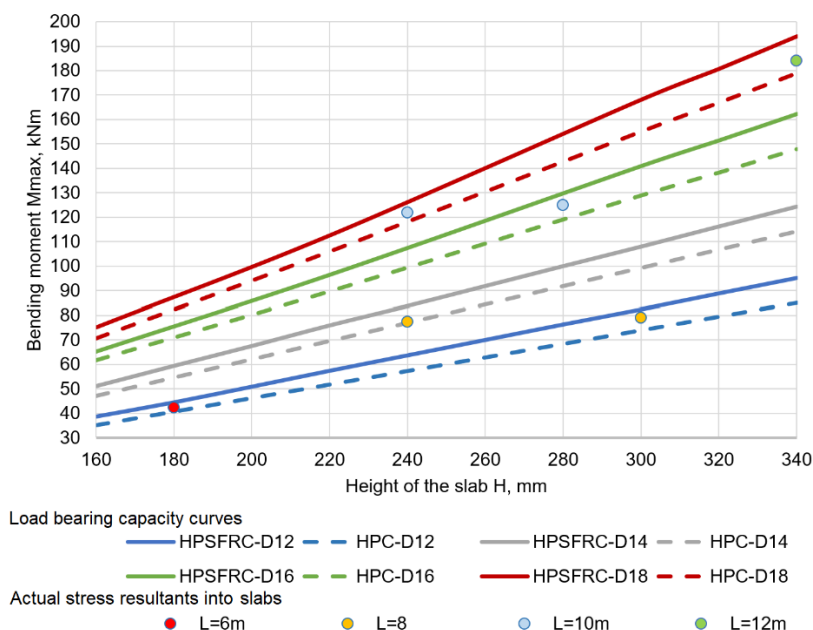


**Figure 10. The dependence of bending moment in the middle of the span on the slab height with various bar diameter for HPC and HPSFRC. HPSFRC is high-performance steel fibre reinforced concrete; HPC is high-performance concrete,  $D$  is bar diameter.**

Taking into account the obtained relationships for determining the width of the ribs and the thickness of the web, curves that describe the load bearing capacity of the slabs dependence of the slab height have been developed. Maximum bending moment in the middle of the slab is determined for the slabs with various heights and bars diameters of the ribs. The spans of the slabs are equal to 6, 8, 10 and 12 m (Figure 10).

It can be seen from the Figure 10 that differences between the load bearing capacities of the slabs of HPC and HPSFRC additionally longitudinally reinforced, is small. The load bearing capacities of the HPSFRC slabs are 5–10 % greater than that of HPC slabs.

The curves for HPC and HPSFRC slabs with 4 different cross-sections, which describes the value of the distributed load  $q$ , at which deflection ( $\Delta$ ) in the middle of the slab is equal to  $L / 250$  for different slab spans, are summarized on the Figure 11.

The used values of distributed load (permanent and imposed loads) for slabs with span 6, 8, 10 and 12 m are shown on the Figure 11.

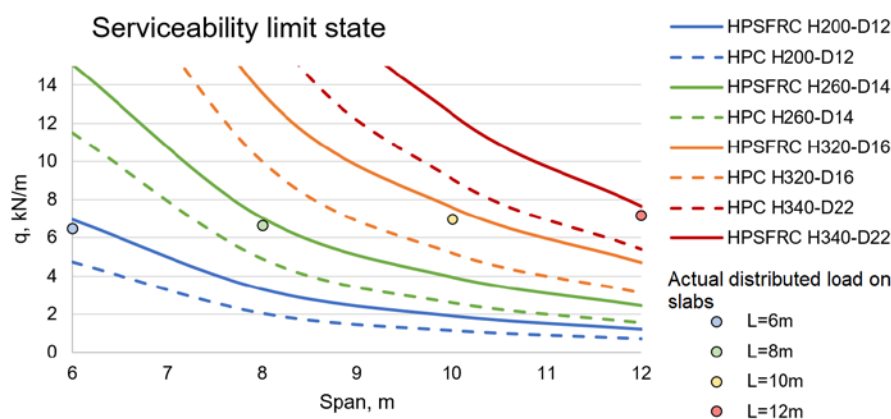


**Figure 11. The dependences of uniformly distributed loads which satisfy the serviceability of the slabs on their spans for different slab height and reinforcement bars diameters for HPC and HPSFRC. HPSFRC is high-performance steel fibre reinforced concrete; HPC is high-performance concrete,  $H$  is slab height,  $D$  is bar diameter.**

It can be concluded, that the slabs made of HPSFRC can take up load which is 42–46 % higher, than that for the slabs made of HPC. The serviceability limit state is determinant so as the intensity of the uniformly distributed load is such that cause the maximum vertical displacements equal to it maximum available value ( $L / 250$ ).

#### 4. Conclusions

Behaviour of HPSFRC and HPC load-bearing members of multi-storey building with columns spacings from 6 to 13 m was compared numerically. Preferable fields of application of high-performance steel fibre reinforced concrete for the load bearing members of considered twelve storey building were justified.

The results showed that:

- HPSFRC columns can take up 40–90 % higher bending moment in comparison with HPC columns at the same level of axial force and parameters of cross-sections, what can be applied for the first eight storeys of considered twelve storeys building with column spacing 8–13 m, where columns characterized by a relatively high bending moment value at a high axial force;
- The using of HPSFRC walls are effective for buildings with the columns spacings changing from 8 to 13 m;
- HPSFRC slab can carry 42–46 % more uniformly distributed load than HPC, for slabs with the same cross-sections and allowed deflection for the spans within limits from 6 to 12 m;
- Dimensions of cross-sections and ratio of longitudinal reinforcement for members subjected to flexure and compression with the bending can be decreased by 10–20 % by using high-performance steel fibre reinforced concrete.

#### 5. Acknowledgements

Financial support: European Regional Development Fund project Nr.1.1.1.1/16/A/007 "A New Concept for Sustainable and Nearly Zero-Energy Buildings".

## References

1. Rigaud, S., Chanvillard, G., Chen, J. Characterization of bending and tensile behavior of ultra-high performance concrete containing glass fibers. RILEM Bookseries. 2012. Vol. 2. Pp. 373–380.
2. Song, P.S., Hwang, S. Mechanical properties of high-strength steel fiber-reinforced concrete. Construction and Building Materials. 2004. Vol.18. Pp. 669–673.
3. Abdul-Razzak, A.A., Mohammed Ali, A.A. Modelling and numerical simulation of high strength fibre reinforced concrete corbels. Applied Mathematical Modelling. 2011. Vol. 35. No. 6. Pp. 2901–2915.
4. Jansson, A., Flansbjerg, M., Löfgren, I., Lundgren, K., Gylltoft, K. Experimental investigation of surface crack initiation, propagation and tension stiffening in self-compacting steel-fibre-reinforced concrete. Materials and Structures/Materiaux et Constructions. 2012. Vol. 45. No. 8. Pp. 1127–1143.
5. Yusof, M.A., Nor, N.M., Zain, M.F.M., etc. Mechanical properties of hybrid steel fibre reinforced concrete with different aspect ratio. Australian Journal of Basic and Applied Sciences. 2011. Vol.5. No.7. Pp.159–166.
6. Bhargava, P., Sharma, U.K., Kaushik, S.K. Compressive stress-strain behaviour of small scale steel fibre reinforced high strength concrete cylinders. Journal of Advanced Concrete Technology. 2006. Vol.4. No.1. Pp. 109–121.
7. Klyuev, S.V., Klyuev, A.V., Abakarov, A.D., Shorstova, E.S., Gafarova, N.G. The effect of particulate reinforcement on strength and deformation characteristics of fine-grained concrete. Magazine of Civil Engineering. 2017. Vol.75. No. 7. Pp. 66–75.
8. Olivito, R.S., Zuccarello, F.A. An experimental study on the tensile strength of steel fiber reinforced concrete. Composites: Part B. 2010. Vol. 41. Pp. 246–255.
9. Keyvani Someh, A., Saeki, N. Prediction for the stress-strain curve of steel fiber reinforced concrete. Transactions of the Japan Concrete Institute. 1996. Vol.18. Pp. 175–182.
10. Aydin S. Effects of fiber strength on fracture characteristics of normal and high strength concrete. Periodica Polytechnica Civil Engineering. 2013. Vol. 57. No. 2. Pp. 191–200.
11. Singh, H. Steel fiber reinforced concrete – behavior, modelling and design. Ludhiana: Springer, 2017, 172 p.
12. Kazemi, M.T., Golsorkhtabar, H., Beygi, M.H.A., Gholamitabar, M. Fracture properties of steel fiber reinforced high strength concrete using work of fracture and size effect methods. Construction and Building Materials. 2017. Vol. 142. Pp. 482–489.
13. Ulas, M.A., Alyamac, K.E., Ulucan, Z.C. Effects of aggregate grading on the properties of steel fibre-reinforced concrete. IOP Conference Series: Materials Science and Engineering. 9th International Conference Fibre Concrete 2017, Prague, Czech Republic, September 13-16, 2017. Vol. 246, No. 1. Article No. 012015.
14. Nikolenko, S.D., Sushko, E.A., Sazonova, S.A., Odnolko, A.A., Manokhin, V.Ya. Behaviour of concrete with a disperse reinforcement under dynamic loads. Magazine of Civil Engineering. 2017. No. 7. Pp. 3–14.
15. Vougioukas, E., Papadatou, M. A model for the prediction of the tensile strength of fiber-reinforced concrete members, before and after cracking. Fibers. 2017. Vol. 5. No. 3. Article No. 27.
16. Simões, T., Octávio, C., Valença, J., Costa, H., Dias-da-Costa D., Júlio, E. Influence of concrete strength and steel fibre geometry on the fibre/matrix interface. Composites Part B: Engineering. 2017. Vol. 122. Pp. 156–164.
17. Balanji, E.K.Z., Sheikh, M.N., Hadi, M.N.S. Behavior of hybrid steel fiber reinforced high strength concrete. Proceedings of the First European and Mediterranean Structural Engineering and Construction Conference

## Литература

1. Rigaud S., Chanvillard G., Chen J. Characterization of bending and tensile behavior of ultra-high performance concrete containing glass fibers // RILEM Bookseries. 2012. Vol. 2. Pp. 373–380.
2. Song P.S., Hwang S. Mechanical properties of high-strength steel fiber-reinforced concrete // Construction and Building Materials. 2004. Vol. 18. Pp. 669–673.
3. Abdul-Razzak A.A., Mohammed Ali A.A. Modelling and numerical simulation of high strength fibre reinforced concrete corbels // Applied Mathematical Modelling. 2011. Vol. 35. № 6. Pp. 2901–2915.
4. Jansson A., Flansbjerg M., Löfgren I., Lundgren K., Gylltoft K. Experimental investigation of surface crack initiation, propagation and tension stiffening in self-compacting steel-fibre-reinforced concrete. Materials and Structures/Materiaux et Constructions. 2012. Vol. 45. № 8. Pp. 1127–1143.
5. Yusof M.A., Nor N.M., Zain, M.F.M., etc. Mechanical properties of hybrid steel fibre reinforced concrete with different aspect ratio // Australian Journal of Basic and Applied Sciences. 2011. Vol. 5. № 7. Pp.159–166.
6. Bhargava P., Sharma U.K., Kaushik S.K. Compressive stress-strain behaviour of small scale steel fibre reinforced high strength concrete cylinders // Journal of Advanced Concrete Technology. 2006. Vol. 4. № 1. Pp. 109–121.
7. Klyuev S.V., Klyuev A.V., Abakarov A.D., Shorstova E.S., Gafarova N.G. The effect of particulate reinforcement on strength and deformation characteristics of fine-grained concrete // Magazine of Civil Engineering. 2017. Vol. 75. № 7. Pp. 66–75.
8. Olivito R.S., Zuccarello F.A. An experimental study on the tensile strength of steel fiber reinforced concrete // Composites: Part B. 2010. Vol. 41. Pp. 246–255.
9. Keyvani Someh A., Saeki N. Prediction for the stress-strain curve of steel fiber reinforced concrete // Transactions of the Japan Concrete Institute. 1996. Vol. 18. Pp. 175–182.
10. Aydin S. Effects of fiber strength on fracture characteristics of normal and high strength concrete // Periodica Polytechnica Civil Engineering. 2013. Vol. 57. № 2. Pp. 191–200.
11. Singh H. Steel fiber reinforced concrete – behavior, modelling and design. Ludhiana: Springer, 2017, 172 p.
12. Kazemi M.T., Golsorkhtabar H., Beygi M.H.A., Gholamitabar M. Fracture properties of steel fiber reinforced high strength concrete using work of fracture and size effect methods // Construction and Building Materials. 2017. Vol. 142. Pp. 482–489.
13. Ulas M.A., Alyamac K.E., Ulucan, Z.C. Effects of aggregate grading on the properties of steel fibre-reinforced concrete // IOP Conference Series: Materials Science and Engineering. 9th International Conference Fibre Concrete 2017, Prague, Czech Republic, September 13–16, 2017. Vol. 246, № 1. Article № 012015.
14. Nikolenko S.D., Sushko E.A., Sazonova S.A., Odnolko A.A., Manokhin V.Ya. Behaviour of concrete with a disperse reinforcement under dynamic loads // Magazine of Civil Engineering. 2017. № 7. Pp. 3–14.
15. Vougioukas E., Papadatou M. A model for the prediction of the tensile strength of fiber-reinforced concrete members, before and after cracking // Fibers. 2017. Vol. 5. № 3. Article № 27.
16. Simões T., Octávio C., Valença J., Costa H., Dias-da-Costa D., Júlio, E. Influence of concrete strength and steel fibre geometry on the fibre/matrix interface // Composites Part B: Engineering. 2017. Vol. 122. Pp. 156–164.
17. Balanji E.K.Z., Sheikh M.N., Hadi M.N.S. Behavior of hybrid steel fiber reinforced high strength concrete // Proceedings of the First European and Mediterranean Structural Engineering and Construction Conference EURO-MED-SEC-1, Istanbul, Turkey, May 24-29, 2016. Pp. 29–34.

- EURO-MED-SEC-1, Istanbul, Turkey, May 24-29, 2016. Pp. 29–34.
18. Travush, V.I., Konin, D.V., Krylov, A.S. Strength of reinforced concrete beams of high-performance concrete and fiber reinforced concrete. Magazine of Civil Engineering. 2018. No. 1. Pp. 90–100.
  19. Savita, Shwetha S., Malanbi, Shweta, Saksheshwari, Manjunath K. Experimental study on strength parameters of steel fiber reinforced concrete using GI wire & fly ash. International Research Journal of Engineering and Technology. 2018. Vol. 5. No. 5. Pp. 3271–3277
  20. Marara, K., Erenb, Ö., Yitmen, İ. Compression specific toughness of normal strength steel fiber reinforced concrete (NSSFRC) and high strength steel fiber reinforced concrete (HSSFRC). Materials Research. 2011. Vol. 14. No. 2. Pp. 239–247.
  21. Neves, R.D., De Fernandes Almeida, J.C.O. Compressive behaviour of steel fibre reinforced concrete. Structural Concrete. 2005. Vol. 6. No. 1. Pp. 1–8.
  22. Li, B., Xu, L., Chi, Y., Huang, B., Li, C. Experimental investigation on the stress-strain behavior of steel fiber reinforced concrete subjected to uniaxial cyclic compression. Construction and Building Materials. 2017. Vol. 140. Pp. 109–118.
  23. ANSYS 12.1 Mechanical APDL Manual. Ansys Inc., 2009.
  24. EN 1992-1-1: Eurocode 2: Design of concrete structures – Part 1-1: General rules and rules for buildings.
  25. Sliseris, J. Numerical analysis of reinforced concrete structures with oriented steel fibers and re-bars // Engineering Fracture Mechanics. 2018. Vol. 194. Pp. 337-349.
  26. Sliseris, J., Yan, L., Kasal, B. Numerical modelling of flax short fibre reinforced and flax fibre fabric reinforced polymer composites // Composites Part B: Engineering. 2016. Vol.89. Pp. 143–154.
  27. Sliseris, J. Numerical estimation of the mechanical properties of a steel-fiber-reinforced geopolymer composite // Mechanics of Composite Materials, 2018. Vol. 54. No. 5. Pp. 1–18.
  28. Sliseris, J., Rocens, K. Rational structure of panel with curved plywood ribs. World Academy of Science, Engineering and Technology: International Conference on Building Science and Engineering (ICBSE 2011), Italy, Venice, April 27-29, 2011. Pp. 317–323.
  29. Sliseris, J., Rocens, K. Optimal design of composite plates with discrete variable stiffness. Composite Structures. 2013. Vol. 98. Pp. 15–23.
  30. RILEM TC 162-TDF: 'Test and design methods for steel fibre reinforced concrete'  $\sigma$ - $\epsilon$ -design method. Materials and Structures/Materiaux et Constructions. 2003. Vol. 36. No. 262. Pp. 560–567.
  18. Travush V.I., Konin D.V., Krylov A.S. Strength of reinforced concrete beams of high-performance concrete and fiber reinforced concrete // Magazine of Civil Engineering. 2018. № 1. Pp. 90–100.
  19. Savita, Shwetha S., Malanbi, Shweta, Saksheshwari, Manjunath K. Experimental study on strength parameters of steel fiber reinforced concrete using GI wire & fly ash. International Research // Journal of Engineering and Technology. 2018. Vol. 5. № 5. Pp. 3271–3277
  20. Marara K., Erenb Ö., Yitmen İ. Compression specific toughness of normal strength steel fiber reinforced concrete (NSSFRC) and high strength steel fiber reinforced concrete (HSSFRC) // Materials Research. 2011. Vol. 14. № 2. Pp. 239–247.
  21. Neves R.D., De Fernandes Almeida J.C.O. Compressive behaviour of steel fibre reinforced concrete // Structural Concrete. 2005. Vol. 6. № 1. Pp. 1–8.
  22. Li B., Xu L., Chi Y., Huang B., Li C. Experimental investigation on the stress-strain behavior of steel fiber reinforced concrete subjected to uniaxial cyclic compression // Construction and Building Materials. 2017. Vol. 140. Pp. 109–118.
  23. ANSYS 12.1 Mechanical APDL Manual. Ansys Inc., 2009.
  24. EN 1992-1-1: Eurocode 2: Design of concrete structures – Part 1-1: General rules and rules for buildings.
  25. Sliseris J. Numerical analysis of reinforced concrete structures with oriented steel fibers and re-bars // Engineering Fracture Mechanics. 2018. Vol. 194. Pp. 337-349.
  26. Sliseris J., Yan L., Kasal B. Numerical modelling of flax short fibre reinforced and flax fibre fabric reinforced polymer composites // Composites Part B: Engineering. 2016. Vol.89. Pp. 143–154.
  27. Sliseris J. Numerical estimation of the mechanical properties of a steel-fiber-reinforced geopolymer composite // Mechanics of Composite Materials, 2018. Vol. 54. № 5. Pp. 1–18.
  28. Sliseris J., Rocens K. Rational structure of panel with curved plywood ribs. World Academy of Science // Engineering and Technology: International Conference on Building Science and Engineering (ICBSE 2011), Italy, Venice, April 27-29, 2011. Pp. 317–323.
  29. Sliseris J., Rocens K. Optimal design of composite plates with discrete variable stiffness // Composite Structures. 2013. Vol. 98. Pp. 15–23.
  30. RILEM TC 162-TDF: 'Test and design methods for steel fibre reinforced concrete'  $\sigma$ - $\epsilon$ -design method // Materials and Structures/Materiaux et Constructions. 2003. Vol. 36. № 262. Pp. 560–567.

*Karina Buka-Vaivade,*  
+37126353082; *karina.buka.vaivade@gmail.com*

*Janis Sliseris,*  
+37126214882; *janis.sliseris@rtu.lv*

*Dmitrijs Serdjuks\*,*  
+37126353082; *Dmitrijs.Serdjuks@rtu.lv*

*Leonids Pakrastins,*  
+37129452138; *leonids.pakrastins@rtu.lv*

*Nikolai Vatin,*  
+79219643762; *vatin@mail.ru*

*Карина Бука-Вайваде,*  
+37126353082;  
*эл. почта: karina.buka.vaivade@gmail.com*

*Янис Шлисерис,*  
+37126214882; *эл. почта: janis.sliseris@rtu.lv*

*Дмитрий Олегович Сердюк\*,*  
+37126353082;  
*эл. почта: Dmitrijs.Serdjuks@rtu.lv*

*Леонид Пакрастиньш,*  
+37129452138; *эл. почта: leonids.pakrastins@rtu.lv*

*Николай Иванович Ватин,*  
+79219643762; *эл. почта: vatin@mail.ru*

© Buka-Vaivade, K., Sliseris, J., Serdjuks, D., Pakrastins, L., Vatin, N.I., 2018

Buka-Vaivade, K., Sliseris, J., Serdjuks, D., Pakrastins, L., Vatin, N.I. Rational use of HPSFRC in multi-storey building. Magazine of Civil Engineering. 2018. 84(8). Pp. 3–14. doi: 10.18720/MCE.84.1.